5.4 Received 5 March 1970

A New Approach to Analysis and Design of Electromechanical Filters by Finite-Element Technique

YUKIO KAGAWA*

Institute of Sound and Vibration Research, University of Southampton, England

Finite-element method was originally developed for analyzing structures such as beams and shells. A flexure-type composite vibrator has been used as an example to illustrate the application of this method to vibration problems involving coupled mechanical and electrical systems [Y. Kagawa and G. M. L. Gladwell, IEEE Trans. Sonics Ultrasonics **SU-17**, No. 1, 41–49 (1970); J. Acoust. Soc. Japan **26**, No. 3, 117–128 (1970)]. This paper develops and adapts this method for the analysis of electromechanical filters of complex shape and construction. The transmission characteristics of a filter are calculated directly without employing the usual method of an equivalent electrical circuit. Two examples of analysis are introduced for presentation. In the first one, the input and output electrodes are set up on the transducers of a composite vibrator, while in the second, two vibrators are coupled by a pair of bars.

LIST OF SYMBOLS

For a Composite Vibrator:

s_{11}^E	compliance at constant E_3
d_{31}	piezoelectric coefficient
ϵ_{33}^T	absolute dielectric constant at constant stress ($\epsilon_0=8.855\times10^{-12}$ in free space)
ϵ	longitudinally clamped permittivity $\epsilon_{33}^T(1-k_{31}^2)$
B	$=k_{31}^2/d_{31}(1-k_{31}^2)$
k_{31}	static longitudinal electromechanical coupling coefficient $k_{31}^2=d_{31}^2/\epsilon_{33}^T s_{11}^E$ $=\epsilon B^2/Y_t$
x, y, z	Cartesian coordinates
ω	angular frequency $\omega=2\pi f$
t	time
$(\ )'$	$\partial/\partial x$ derivative with respect to x
h_m, h_t	half-thickness of resonator and thickness of transducer (suffixes m and t indicate those of resonator and transducer)
Y_m, Y_t	Young's modulus
b_m, b_t	width
ρ_m, ρ_t	density
L	total length of vibrator
l_t	total length of transducer
l_i	length of ith element
r_b	$=b_t/b_m$
r_h	$=h_t/h_m$
r_Y	$=Y_t/Y_m$
r_ρ	$=\rho_t/\rho_m$
r_{L_i}	$=l_i/L$
r_{hL}	$=h_m/L$
r_{bh}	$=b_m/h_m$
$(\Omega)^\natural$	$=\omega L/c_m$
c_m	$=(Y_m/\rho_m)^\natural$
w, ψ	$w=we^{j\omega t}$ and $\psi=\psi e^{j\omega t}$, flexural displacement and slope
w_i, ψ_i	flexural displacement and slope at the ith junction of two elements
V_E	$V_E=V_E e^{j\omega t}$, applied voltage
V_i, M_i	$V_i=V_i e^{j\omega t}$ and $M_i=M_i e^{j\omega t}$, shear force and moment of inertia at the ith junction of two elements
Q_i	electric charge of the ith element
C_i	longitudinally clamped capacitance of the ith element (both sides of the transducers connected in parallel)
I_i	$I_i=\dot{Q}_i=j\omega Q_i$, electric current through the ith element
Y_{M_i}	motional admittance in electric terminals of the ith element
Z_0	characteristic impedance
R_T	termination resistance
A_{TT}	insertion loss (decibels)
α	$=b_m h_m r_b(1+\frac{1}{2}r_h)$
β	$=b_m h_m^3 r_b r_h(1+r_h+\frac{1}{2}r_h^2)$

γ $=\frac{1}{3}b_m h_m^3[1+3r_b r_Y r_h(1+r_h+\frac{1}{3}r_h^2)]$
δ $=\rho_m b_m h_m(1+r_\rho r_b r_h)$

For a Bar Coupler:

s	coordinate in the axial direction of coupler
Y_c	Young's modulus
μ_c	$=Y_c/2(1+\sigma_c)$
ρ_c	density
σ_c	Poisson's ratio
AY_c	flexural rigidity
$C\mu_c$	torsional rigidity
a_c	radius of coupler
L_c	total length of coupler
l_{cj}	length of jth element
r_{Y_c}	$=Y_c/Y_m$
r_{ρ_c}	$=\rho_c/\rho_m$
$r_{L_{cj}}$	$=l_{cj}/L_c$
r_{LL}	$=L_c/L$
r_μ	$=\mu_c/Y_m=r_{Y_c}/2(1+\sigma_c)$
r_{aL}	$=a_c/L_c$
c_c	$=(Y_c/\rho_c)^{\frac{1}{2}}$
v, ϕ, θ	$v=ve^{j\omega t}$, $\phi=e^{j\omega t}$, and $\theta=\theta e^{j\omega t}$, flexural displacement, slope, and rotation around the axis
v_j, ϕ_j, θ_j	displacement, slope, and rotation around the axis at the jth junction
R_j, N_j, G_j	$R_j=R_j e^{j\omega t}$, $N_j=N_j e^{j\omega t}$, and $G_j=G_j e^{j\omega t}$, shear force, moment, and torsion around the axis at jth junction

INTRODUCTION

The analysis and design of electromechanical vibrators and filters are usually carried out by obtaining their equivalent electrical circuits within their resonant frequency ranges.[1] In the filters making use of the extensional or torsional vibrations of bars or cylinders, this treatment is noted for its simplicity. The equivalent electrical circuits in such cases can be written in terms of a four-terminal network, as long as their vibrational systems can reasonably be considered as one-dimensional. Thus, a well-established four-terminal network theory[2,3] can be utilized.

Filters making use of the flexural vibrations of beams and plates are interesting because of their compact construction.[4,5] Konno and his colleagues[6] have developed an equivalent electrical circuit for flexural vibration of a beam. However, the resulting eight-terminal circuit is complicated, because it must include rotations and slopes of the beam as well as the corresponding stresses and displacements.

The author and his colleague[7,8] have developed a new analytical technique for a flexure-type vibrator, making use of the finite-element method. This technique turns out to be a powerful means for the analysis and design of electromechanical vibrators and filters of complex shape and construction. This paper describes the application of this finite-element technique to the electromechanical filters. Two examples of analysis are introduced for presentation: (1) a composite vibrator filter with the input and output electrodes on the same transducers and (2) a more advanced filter with two vibrators connected by a pair of bar couplers. The method is quite straightforward and can deal with filters of arbitrary shape and construction without considering the equivalent electrical circuit. It is suitable for use in computer-aided design.[9]

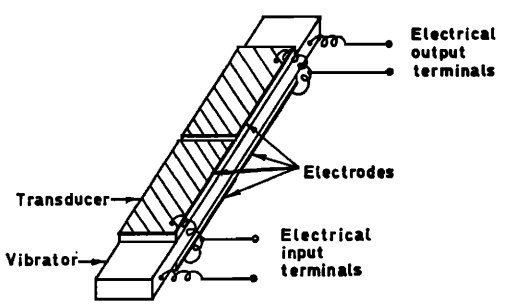

FIG. 1. An example of electromechanical filters with electrostrictive transducers of partial electrodes.

I. A FLEXURE-TYPE VIBRATOR SANDWICHED BETWEEN ELECTROSTRICTIVE TRANSDUCERS

A. Stiffness Matrix

The electromechanical filters to be analyzed here incorporate a flexure-type composite vibrator in which a beam is sandwiched between electrostrictive transducers. A general view of a single vibrator filter is shown in Fig. 1. Figures 2 and 3 show a general view and details, respectively, of a coupled vibrator filter. P and E_3 in the figure indicate the electric polarization and field, respectively, in the electrostrictive material. With electromotive force applied to the properly arranged electrodes, one transducer expands in the x direction while the other contracts. Thus, flexural vibrations develop.

In the case of the vibrator filter shown in Fig. 1, the electrodes on the transducers are arranged into two

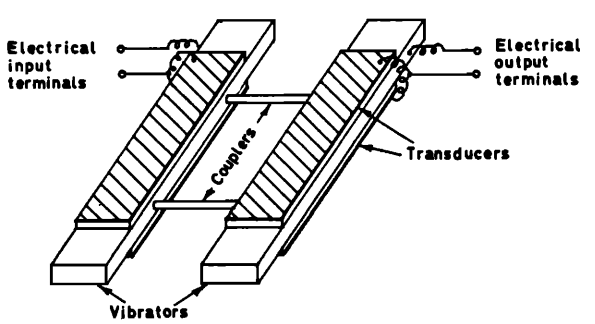

FIG. 2. An example of electromechanical filters with electrostrictive transducers, two vibrators coupled with torsional couplers (after Konno[10]).

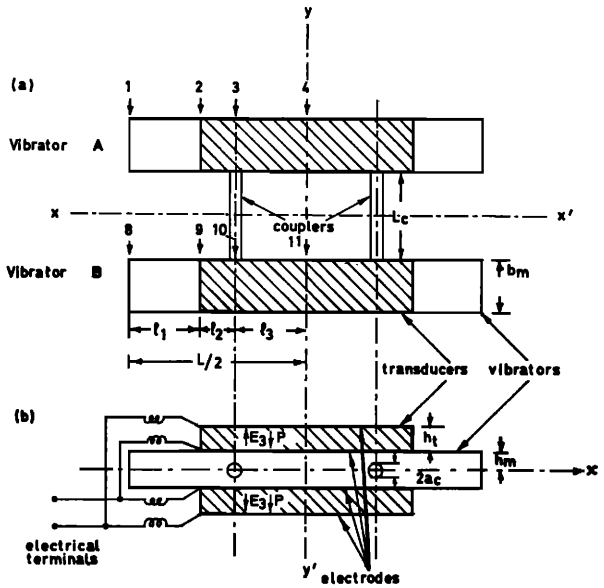

FIG. 3. Top and cross-sectional views of the electromechanical filter in Fig. 2.

parts so that one is input and the other output. When the vibrators are connected with bar couplers as shown in Fig. 2, the rotation and the transverse vibration of one vibrator get transmitted to the other vibrator through torsional and bending motions of the bar couplers. If the couplers are connected at the flexural nodes of the vibrators, the vibrations are transmitted only through the torsion of the couplers.

Referring to the previous analysis,[7,8] one may express the displacement in the ith element of the arbitrarily divided beam as follows:

$$w=L\mathbf{X}^T\mathbf{d}=L[f_1,r_{L_i}f_2,f_3,r_{L_i}f_4]\begin{bmatrix}w_{i-1}/L\\ \psi_{i-1}\\ w_i/L\\ \psi_i\end{bmatrix}; \quad (1)$$

$f_1\sim f_4$ are the displacement functions for the finite-element method (see List of Symbols and Fig. 4).

The relation between the force vector $\mathbf{P}$ and the displacement vector $\mathbf{d}$ at the two ends of the ith element is

$$\mathbf{P}=\mathbf{S}^{(i)}\mathbf{d}, \quad (2)$$

where

$$\mathbf{P}=\mathbf{F}+\mathbf{V}_E=\begin{bmatrix}V_{i-1}\\ M_{i-1}/L\\ V_i\\ M_i/L\end{bmatrix}+\begin{bmatrix}0\\ \alpha\epsilon BV_E/L\\ 0\\ -\alpha\epsilon BV_E/L\end{bmatrix} \quad (3)$$

and

$$\mathbf{S}^{(i)}=2L[(-\beta\epsilon B^2+\gamma Y_m)(1/l_i^3)\mathbf{H}-\omega^2\delta l_i\mathbf{J}]. \quad (4)$$

Matrices $\mathbf{H}$ and $\mathbf{J}$, along with all others which follow in the text of the paper, are introduced in Appendix A. The first term $\mathbf{F}$ in Eq. 3 indicates the shear forces (V_{i-1},V_i) and the moments (M_{i-1},M_i) on the two ends (x_{i-1},x_i) of the ith element. The second term $\mathbf{V}_E$ indicates the electromotive force applied works out as the moments on the two ends. In Eq. 4, $\mathbf{S}^{(i)}$ is the stiffness matrix. The first term $-\beta\epsilon B^2$ is caused by the piezoelectric effect of the transducers, which effectively reduces the stiffness of the composite beam. In elements without transducers, $r_h=r_b=0$.

When the electrical terminals are short-circuited,

$$\mathbf{P}=\mathbf{F}, \quad \text{for } V_E=0.$$

Also, when they are open,

$$I_i=0.$$

The term of electric charge

$$\mathbf{S}_D{}^{(i)}=2L\alpha\epsilon B^2(h_ih_m/l_i^3)(1+\tfrac{1}{2}r_h)\mathbf{D} \quad (5)$$

is to be added to Eq. 4 in this case.

B. Input Admittance

The input admittance of the ith element at the electrical terminals is given as[7,8]

$$Y_i=j\omega C_i+Y_{M_i}, \quad (6)$$

where

$$Y_{M_i}=-j(\Omega)^{\frac{1}{2}}c_mb_mh_ih_m^2r_b(1+\tfrac{1}{2}r_h)^2k_{31}^2Y_tC_i \times\frac{1}{l_iL^2}\left(\frac{\psi_i}{m}-\frac{\psi_{i-1}}{m}\right). \quad (7)$$

This is a parallel circuit of the damped capacitance C_i and the motional admittance Y_{M_i} for the ith element. The total input admittance is

$$Y_0=\sum_i C_i+\sum_i Y_{Mi}, \quad (8)$$

where $\sum_i$ means the summation for all the elements with the transducers provided.

II. COUPLERS

A. Potential Energy and Kinetic Energy

In coupled-vibrator filters as shown in Fig. 2, where vibrators are connected with couplers, the latter may be treated like the former. The jth element of a coupler is shown in Fig. 5. In Konno's case,[10] the couplers are

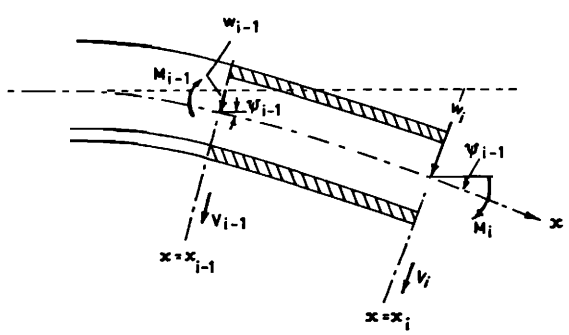

FIG. 4. Forces and moments on an element of a vibrator.

connected to the flexural nodal points of the lowest mode of the vibrator so that transmission is through the torsion of the couplers. This paper deals with a more general case, namely, when the couplers are connected at arbitrary points on the beam, and both torsional and bending vibrations must be taken into account.

When a coupler is very thin, however, the torsional and bending vibrations could be treated without considering their mutual coupling.[11] Then the potential energy and the kinetic energy are expressed as follows:

$$U_c=U_{cf}+U_{ct}=\frac{1}{2}\int_{s_{j-1}}^{s_j} AY_c\left(\frac{\partial^2 v}{\partial s^2}\right)^2 ds + \frac{1}{2}\int_{s_{j-1}}^{s_j} C\mu_c\left(\frac{\partial\theta}{\partial s}\right)^2 ds \quad (9)$$

and

$$T_c=T_{cf}+T_{ct}=\frac{1}{2}\int_{s_{j-1}}^{s_j} \rho_c I_c\left(\frac{\partial v}{\partial t}\right)^2 ds + \frac{1}{2}\int_{s_{j-1}}^{s_j} \rho_c I_{ct}\left(\frac{\partial\theta}{\partial t}\right)^2 ds. \quad (10)$$

The first term represents the bending energy and the second the torsional energy. AY_c is bending rigidity, $C\mu_c$ torsional rigidity, I_c the cross-sectional area, and I_{ct} the moment of inertia about the axis.

B. Stiffness Matrix

The displacement of the flexural vibration of the jth element of the bar is written as follows:

$$v=L_c\mathbf{X}^T\mathbf{g}=L_c[f_1, r_{L_{cj}}f_2, f_3, r_{L_{cj}}f_4]\begin{bmatrix} v_{j-1}/L_c \\ \phi_{j-1} \\ v_j/L_c \\ \phi_j \end{bmatrix}. \quad (11)$$

The potential energy is then

$$U_{cf}=\tfrac{1}{2}AY_c(L_c^2/l_{cj}^3)\mathbf{g}^T\mathbf{H}_c\mathbf{g}, \quad (12)$$

where $\mathbf{H}_c=\mathbf{U}_c\bar{\mathbf{H}}\mathbf{U}_c$. The torsional angle for the same element is

$$\theta=\mathbf{X}_\theta{}^T\boldsymbol{\theta}=[f_{\theta 1}, f_{\theta 2}]\begin{bmatrix}\theta_{j-1}\\ \theta_j\end{bmatrix}, \quad (13)$$

where $f_{\theta 1}=1-y$ and $f_{\theta 2}=y$; $y=(s-s_{j-1})/l_{cj}$ (see Ref. 12). One has the torsional energy

$$U_{ct}=\tfrac{1}{2}C\mu_c(1/l_{cj})\boldsymbol{\theta}^T\mathbf{K}\boldsymbol{\theta}. \quad (14)$$

Similarly, the kinetic energy of the flexural motion is

$$T_{cf}=\tfrac{1}{2}\rho_c I_c\omega^2 L_c{}^2 l_{cj}\mathbf{g}^T\mathbf{J}_c\mathbf{g}, \quad (15)$$

where

$$\mathbf{J}_c=\mathbf{U}_c\bar{\mathbf{J}}\mathbf{U}_c,$$

and the kinetic energy of the torsional motion is

$$T_{ct}=\tfrac{1}{2}\rho_c I_{ct}\omega^2 l_{cj}\boldsymbol{\theta}^T\mathbf{M}\boldsymbol{\theta}. \quad (16)$$

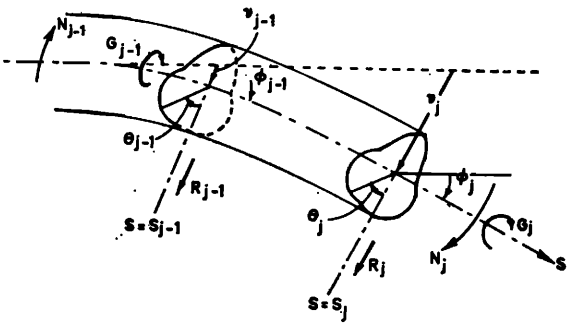

FIG. 5. Forces, moments, and rotations on an element of the coupler of thin rod.

The work done by the external forces at the boundary ends of the jth element is

$$L_c\mathbf{g}^T\mathbf{F}_c=L_c[v_{j-1}/L_c, \phi_{j-1}, v_j/L_c, \phi_j]\begin{bmatrix} R_{j-1} \\ N_{j-1}/L_c \\ R_j \\ N_j/L_c \end{bmatrix} \quad (17)$$

for the flexural motion, and

$$\boldsymbol{\theta}^T\mathbf{G}=[\theta_{j-1}, \theta_j]\begin{bmatrix}G_{j-1}\\ G_j\end{bmatrix} \quad (18)$$

for the torsional motion. Therefore, the relations between the force vectors and the displacement vectors are

$$\mathbf{F}_c=\mathbf{S}_g\mathbf{g} \quad (19)$$

and

$$\mathbf{G}=\mathbf{S}_\theta\boldsymbol{\theta}; \quad (20)$$

$\mathbf{S}_g$ and $\mathbf{S}_\theta$ are the stiffness matrices for the flexural and torsional motion respectively, that is,

$$\mathbf{S}_g=L_c\left(AY_c\frac{1}{l_{cj}{}^3}\mathbf{H}_c-\rho_c I_c\omega^2 l_{cj}\mathbf{J}_c\right) \quad (21)$$

and

$$\mathbf{S}_\theta=\frac{1}{2}\left(C\mu_c\frac{1}{l_{cj}}\mathbf{K}-\rho_c I_{ct}\omega^2 l_{cj}\mathbf{M}\right). \quad (22)$$

The total stiffness matrix for the coupler is

$$\left[\begin{array}{c}\mathbf{F}_c\\ \hline \mathbf{G}\end{array}\right]=\left[\begin{array}{c|c}\mathbf{S}_g & 0\\ \hline 0 & \mathbf{S}_\theta\end{array}\right]\left[\begin{array}{c}\mathbf{g}\\ \hline \boldsymbol{\theta}\end{array}\right]. \quad (23)$$

Equation 20 can be written as follows:

$$\begin{bmatrix}G_{j-1}\\ G_j\end{bmatrix}=\begin{bmatrix}S_{\theta 11} & S_{\theta 12}\\ S_{\theta 21} & S_{\theta 22}\end{bmatrix}\begin{bmatrix}\theta_{j-1}\\ \theta_j\end{bmatrix}. \quad (24)$$

If the bar coupler is symmetrical with respect to the cross section, $S_{\theta 11}=S_{\theta 22}$ and $S_{\theta 12}=S_{\theta 21}$. Therefore, the static stiffness (at $\omega=0$) is

$$S_c=\frac{G_{j-1}-G_j}{\theta_{j-1}-\theta_j}=S_{\theta 11}-S_{\theta 12}=C\mu_c\frac{1}{l_{cj}}. \quad (25)$$

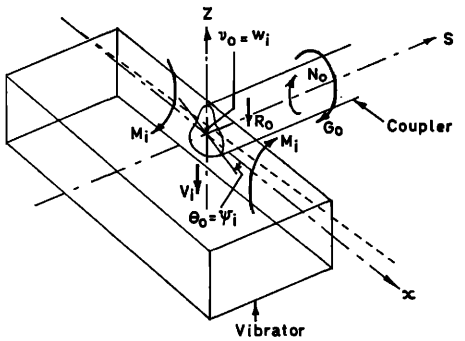

FIG. 6. Connection of the coupler to the vibrator.

When the coupler is of the circular cross section,

$$S_c=\tfrac{1}{2}\pi a_c^4\mu_c(1/l_{cj}). \tag{26}$$

As one would expect, this agrees with Konno's results.[10]

III. COMPATIBILITY

The compatibility at the ith junction between two elements I and II of the vibrator is

$$w_{i\mathrm{I}}=w_{i\mathrm{II}}, \quad \psi_{i\mathrm{I}}=\psi_{i\mathrm{II}} \tag{27}$$

for the displacement vector, and

$$V_{i\mathrm{I}}+V_{i\mathrm{II}}=0, \quad M_{i\mathrm{I}}+M_{i\mathrm{II}}=0 \tag{28}$$

for the force vector.

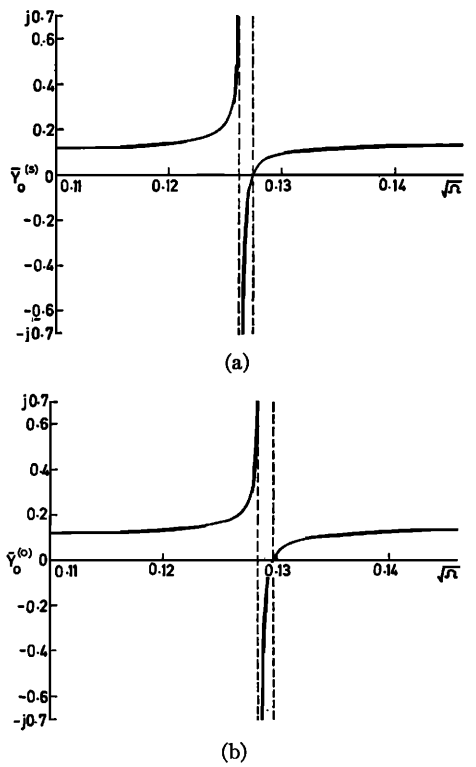

FIG. 7. Normalized input admittance of vibrator filter. (a) Output terminals short-circuited. (b) Output terminals open.

Similarly, at the jth junction of the coupler,

$$v_{j\mathrm{I}}=v_{j\mathrm{II}}, \quad \phi_{j\mathrm{I}}=\phi_{j\mathrm{II}}, \quad \theta_{j\mathrm{I}}=\theta_{j\mathrm{II}}, \tag{29}$$

and

$$R_{j\mathrm{I}}+R_{j\mathrm{II}}=0, \quad N_{j\mathrm{I}}+N_{j\mathrm{II}}=0, \quad G_{j\mathrm{I}}+G_{j\mathrm{II}}=0. \tag{30}$$

At the connection of the coupler to the vibrator, as shown in Fig. 6,

$$v_1=w_{i\mathrm{I}}=w_{i\mathrm{II}}, \quad \theta_1=\psi_{i\mathrm{I}}=\psi_{i\mathrm{II}} \tag{31}$$

and

$$R_1+V_{i\mathrm{I}}+V_{i\mathrm{II}}=0, \quad G_1+M_{i\mathrm{I}}+M_{i\mathrm{II}}=0. \tag{32}$$

Furthermore, one has to consider the boundary conditions for ϕ and N of the coupler, that is, (1) when the coupler is built into the vibrator,

$$\phi_1=0, \tag{33}$$

and (2) when the coupler is hinged to the vibrator,

$$N_1=0. \tag{34}$$

IV. TRANSMISSION CHARACTERISTICS BETWEEN INPUT AND OUTPUT TERMINALS

With the compatibility and the equilibrium conditions being applied to the connections between the elements, one has simultaneous algebraic equations with a coefficient matrix, that is, the stiffness matrix of the whole system which is built up from $\mathbf{S}^{(s)}$, $\mathbf{S}_\rho$, and $\mathbf{S}_\theta$ discussed above. By solving the equations on proper boundary conditions, one may obtain the displacement vectors for an arbitrary frequency parameter Ω. Then the input admittance Y_0 is calculated by means of the ψ_i obtained.

Electromechanical filters (as shown in Figs. 1 and 2) form a four-terminal network with respect to their input and output terminals. The transmission characteristics are then determined by the image impedance and the propagation constant obtained. The input admittances of the vibrator when the secondary terminals are short-circuited and open, respectively, are as follows:

$$Y_0^{(s)}=C_e+\sum_i Y_{M_i}^{(s)}$$

and

$$Y_0^{(0)}=C_e+\sum_i Y_{M_i}^{(0)}, \tag{35}$$

where C_e is the total damped capacitance in the primary terminals, and $Y_{M_i}^{(s)}$ and $Y_{M_i}^{(0)}$ are the motional admittances of the ith element when the secondary terminals are short-circuited and open, respectively. As it is well known, the image impedance at the primary terminals is

$$Z_{01}=1/Y_{01}=1/(Y_{01}^{(s)}Y_{01}^{(0)})^{\frac{1}{2}}. \tag{36}$$

The same procedure can be followed for the secondary terminals (Z_{02}). If the system is symmetrical, as in the

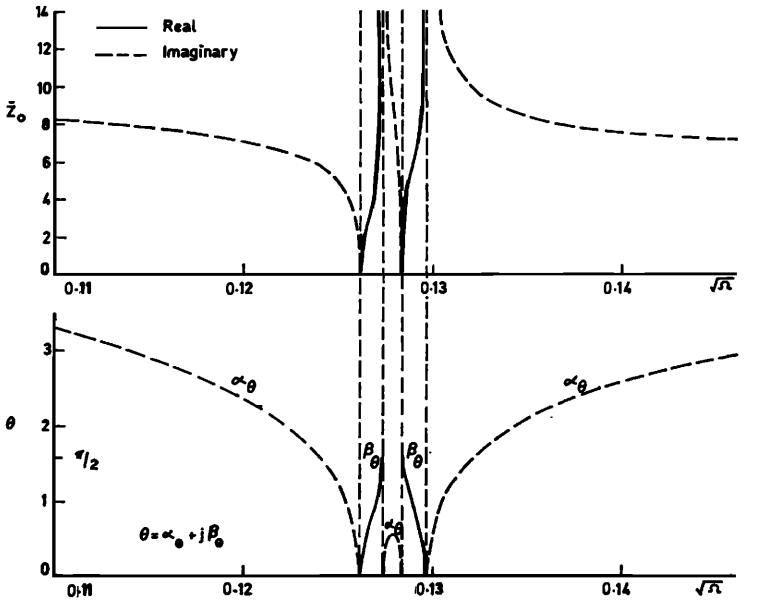

FIG. 8. Normalized characteristic impedance and propagation constant of vibrator filter.

present case, $Z_{01}=Z_{02}=Z_0$, $Y_{01}^{(s)}=Y_{02}^{(s)}=Y_0^{(s)}$, and $Y_{01}^{(0)}=Y_{02}^{(0)}=Y_0^{(0)}$. The propagation constant is then

$$\theta=\alpha_\theta+j\beta_\theta=\tanh^{-1}\left[\frac{Y_0^{(0)}}{Y_0^{(s)}}\right]^{\frac{1}{2}}, \tag{37}$$

where α_θ is the attenuation constant and β_θ is the phase constant.

When the input and the output are terminated with the resistance R_T, the transmission loss[2] is given below (in decibels):

$$A_{TT}=8.686\left[\alpha_\theta+2\log_\epsilon\left|\frac{R_T+Z_0}{2(R_TZ_0)^{\frac{1}{2}}}\right|+\log_\epsilon\left|1-\epsilon^{-2\theta}\left(\frac{Z_0-R_T}{Z_0+R_T}\right)^2\right|\right]. \tag{38}$$

In our present example, the normalized input admittance of the filter for the left-hand side (in Figs. 1 and 2) is

$$\bar{Y}_0=\frac{Y_0L}{c_mC_e}=j(\Omega)^{\frac{1}{2}}\left[1+r_br_hr_Yr_{hL}{}^2k_{31}{}^2\left(1+\frac{1}{2}r_h\right)^2\times\frac{2L}{l_t}\sum_i\left(\frac{\psi_{i-1}}{\bar{m}}-\frac{\psi_i}{\bar{m}}\right)\right], \tag{39}$$

where

$$C_e=\sum_i C_i=\sum_i (2\epsilon b_il_i/h_t),$$

the damped capacitance at the input terminals for the half-length of the vibrator and $\bar{m}=m/h_mb_mY_m$. Thus the input admittances $\bar{Y}_0^{(s)}$ and $\bar{Y}_0^{(0)}$ can be calculated.

V. COMPUTED RESULTS

The accuracy of the natural frequencies of the composite vibrator (two-terminal device) was discussed for the cases of 2 and 10 elements in a previous paper.[8] The maximum percent error of the two-element case is only 0.83 for the fundamental mode of interest here. Therefore, if one divides the half-length of the vibrator into three elements, it will bring satisfactory results.

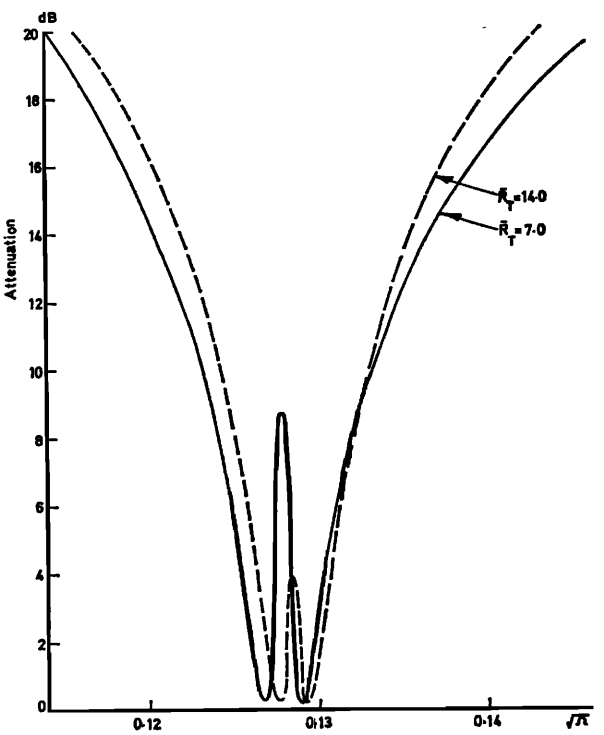

FIG. 9. Transmission characteristics of vibrator filter.

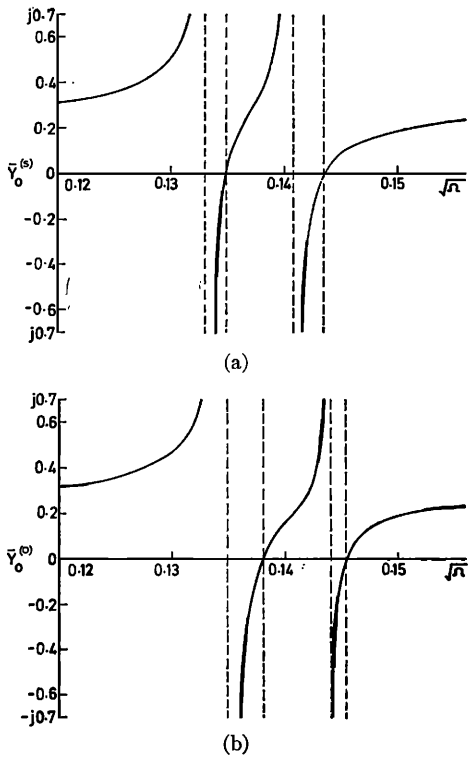

FIG. 10. Normalized input admittance of the filter of two vibrators coupled by torsional rods. (a) Output terminals short-circuited. (b) Output terminals open.

The characteristics of the vibrator filter (as shown in Fig. 1) are first computed, where the electrodes on the transducers are divided into two parts so that one is input and the other output. The vibrator is divided into six elements, three for the left-hand side and three for the right. The dimension of the stiffness matrix is 14×14 for the free–free boundary conditions. The dimensions of the vibrator are as follows: $r_b=1.0$, $r_h=1.5$, $r_{hL}=0.004903$, $r_\rho=0.962$, $r_Y=0.381$, $k_{31}=0.31$, $l_i/L=0.7$, $l_1/L=0.15$, $l_2/L=0.15$, and $l_3/L=0.2$. The normalized input admittances $\bar{Y}_0^{(s)}$ and $\bar{Y}_0^{(0)}$ when the secondary terminals are short-circuited and open are shown in Fig. 7. No stray bridge capacitance between the input and output electrodes is taken into account. The characteristic impedance (image impedance) and the propagation constant calculated are shown in Fig. 8, in which the solid lines indicate the passband and the broken lines the stop band. The insertion loss is calculated by Eq. 38 for the resistance termination $\bar{R}_T=R_TL/c_mC_e$. This is shown in Fig. 9, which shows the double-peak characteristic. This could be made less peaky by employing a tuning-circuit termination. This is, however, beyond the scope of the present discussion.

The electromechanical filter as shown in Fig. 2 remains to be discussed. Since the system is symmetrical with respect to y–y' axis in Fig. 3, only the left-hand side is considered for computation. The vibrator is divided into three parts at the points indicated with arrows in the figure. The numbers associated with these arrows are used for the suffices of the shear force, the displacement, and other quantities at these points. The length of the coupler is so short that it is treated as one element. The boundary conditions are free at one end and sliding at the other (at the center of the vibrator); that is,

$$V_1=M_1=V_8=M_8=0$$

and

$$V_4=\psi_4=V_{11}=\psi_{11}=0.$$

On the other hand, the coupler may be built into the vibrator as in ordinary construction. Then,

$$\phi_3=\phi_{10}=0.$$

On the above boundary conditions, the dimension of

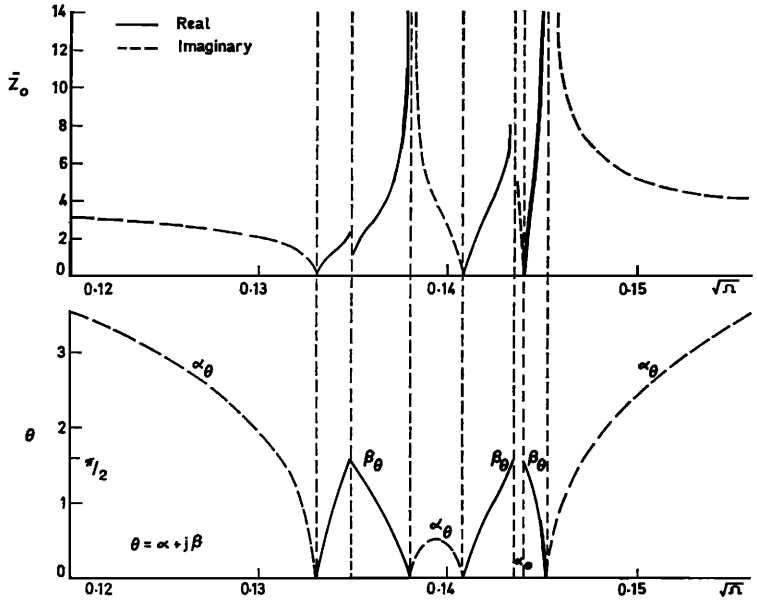

FIG. 11. Normalized characteristic impedance and propagation constant of the filter of two vibrators coupled by torsional rods.

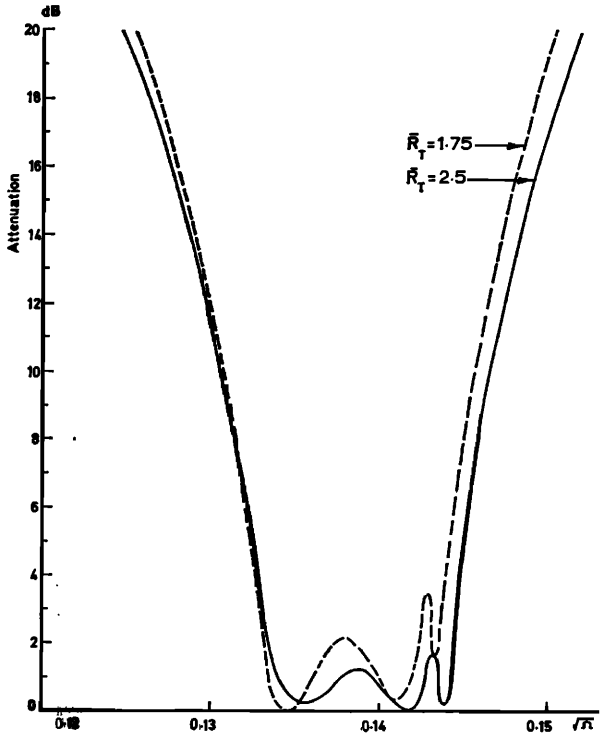

FIG. 12. Transmission characteristics of the filter of two vibrators coupled by torsional rods.

the stiffness matrix is finally 14×14. In the particular case when the couplers are connected to the vibrators at their nodal points, the element $\mathbf{S}_g$ can be neglected. With reference to Kusakabe's findings,[13] the dimensions of the filter are chosen as follows, except for those in our previous case: (1) $r_{hL}=0.005171$, $r_{bh}=25.0$, $l_2/L=0.113$, and $l_3/L=0.237$ for the vibrator, and (2) $r_{L_{c1}}=1.0$ (one element), $r_{LL}=0.1608$, $r_{aL}=0.0643$, $r_{\rho c}=1.0$, $r_\mu=0.381$, and $r_{Yc}=1.0$ for the coupler.

The input admittances when the secondary terminals are short-circuited and open are shown in Fig. 10. (The values shown have been doubled for full length of the vibrators.) The characteristic impedance, the propagation constant, and the insertion loss are shown in Figs. 11 and 12. The passband is wider than the previous example, as expected.

VI. DISCUSSION

As seen in Fig. 10, there are two resonances for each of the cases (a) and (b). The frequency parameters are $(\Omega)^{\frac{1}{2}}=0.1331$ and 0.1408 for the former and $(\Omega)^{\frac{1}{2}}=0.1348$ and 0.1440 for the latter. The vibrational modes at these frequencies are shown in Figs. 13 and 14. When the output terminals are short-circuited, the vibrators move in phase in the lower resonance. The resonant frequency is not affected by the presence of the couplers. The motion is out of phase in the higher resonance and the resonant frequency increases because of the stiffness of the couplers. The modal shape is symmetrical for

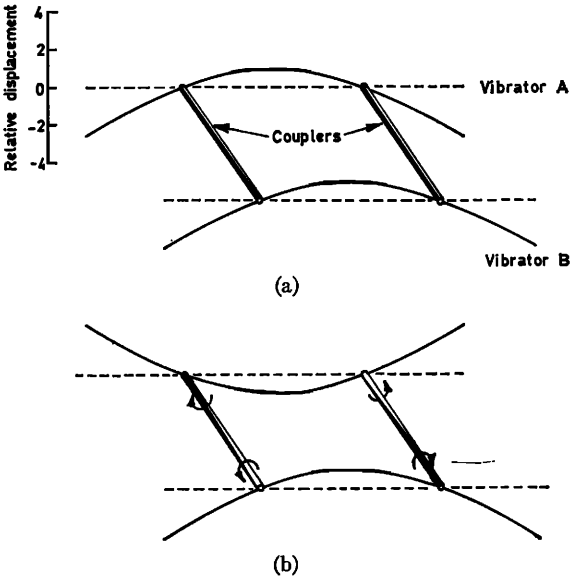

FIG. 13. Mode shape of the filter at resonances when output terminals (Vibrator B) are short-circuited. (a) In phase, $(\Omega)^{\frac{1}{2}}=0.1331$. (b) Out of phase, $(\Omega)^{\frac{1}{2}}=0.1408$.

both input and output vibrators. When the output terminals are open, on the other hand, the modal shape is not symmetrical and the resonant frequencies slightly increase for both in-plane and out-of-plane modes.

Comparison was made between the two transmission characteristics obtained by neglecting and including the flexural stiffness of the couplers. No noticeable difference was found. This is explained by the particular positions of the coupler's connection to the vibrators.

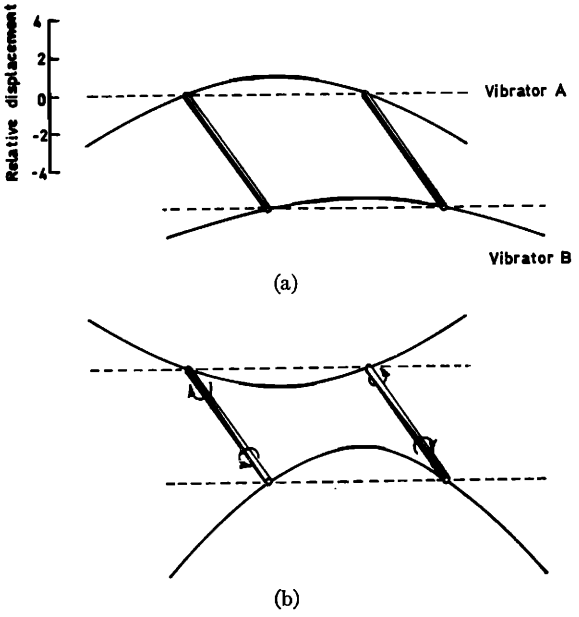

FIG. 14. Mode shape of the filter at resonances when output terminals (Vibrator B) are open. (a) In phase, $(\Omega)^{\frac{1}{2}}=0.1348$. (b) Out of phase, $(\Omega)^{\frac{1}{2}}=0.1440$.

All the dimensions of this filter were taken from the work of Kusakabe,[13] who intentionally chose the flexural nodes of the vibrator for the coupler's connection. In our computation, the displacements at these points are of the order of 10^{-2} times the maximum displacement. This effectively makes these points the flexural nodes of the vibrator. From the transmission characteristics in Fig. 12, the center frequency parameter and the bandwidth are $(\Omega_c)^{\frac{1}{2}}=0.139$ (0.1405) and $\Delta\Omega=0.01$ (0.0093); then $(\Delta f/f_c)=[\Delta\Omega/(\Omega_c)^{\frac{1}{2}}]=0.072$ (0.667). The figures in the brackets show corresponding results obtained by Kusakabe employing equivalent electrical circuit treatment. (His computation, however, utilizes the measured values of the effective mass of the vibrator and the force factor.)

The technique reported in this paper for calculating the characteristics of electromechanical filters by the finite-element method is straightforward. Theoretically, the electromechanical filters of any complicated shape and construction could be treated by this method by dividing the physical configuration properly. The method is not directly suitable for synthesis, but is adaptable for iteration technique.

ACKNOWLEDGMENTS

The author is grateful to Professor G. M. L. Gladwell, University of Waterloo, Canada, for his encouragement and many helpful comments. Acknowledgments are also due to K. K. Pujara, Indian Institute of Technology, New Delhi, for some discussions and for rephrasing some parts of the text. The work reported here was carried out under a grant of the Science Research Council.

* At present, the author is with the Department of Electrical Engineering, Toyama University, Japan.

[1] W. P. Mason, *Electromechanical Transducers and Wave Filters* (Van Nostrand, Princeton, N. J., 1948).
[2] K. Nagai and R. Kamiya, *Transmission Network Theory* (Corona-sha, Tokyo, 1956), Vol. I.
[3] J. L. Potter and S. J. Fich, *Theory of Networks and Lines* (Prentice-Hall, Englewood Cliffs, N. J., 1963).
[4] K. Yakuwa and S. Okuda, "Miniaturization of the Mechanical Vibrator Used in an Electromechanical Filter," Rep. Int. Congr. Acoust., 6th, Tokyo (1968), paper 6-3-5.
[5] W. P. Mason and R. N. Thurston, "A Compact Electromechanical Bandpass Filter for Frequencies below 20 Kilocycles," IRE Trans. Ultrasonics Eng. **UE-7**, 59–70 (1960).
[6] M. Konno and H. Nakamura, "Equivalent Electrical Network for the Transversely Vibrating Uniform Bar," J. Acoust. Soc. Amer. **38**, 614–622 (1965).
[7] Y. Kagawa and G. M. L. Gladwell, "Finite Element Analysis of Flexure-Type Vibrators with Electrostrictive Transducers," IEEE Trans. Sonics Ultrasonics **SU-17**, No. 1, 41–49 (1970).
[8] Y. Kagawa and G. M. L. Gladwell, "Application of a Finite Element Method to Vibrational Problems in which Electrical and Mechanical Systems are Coupled," J. Acoust. Soc. Japan **26**, No. 3, 117–128 (1970).
[9] G. L. Smith, "Computer-Aided Filter Design," Can. Electron. Eng. 42–46 (April 1969).
[10] M. Konno, C. Kusakabe, and Y. Tomikawa, "Electromechanical Filter Composed of Transversely Vibrating Resonators for Low Frequencies," J. Acoust. Soc. Amer. **39**, 953–961 (1966).
[11] A. E. H. Love, *Treatise on the Mathematical Theory of Elasticity* (Cambridge U. P., London, 1927), p. 232.
[12] G. M. L. Gladwell, "The Vibration of Mechanical Resonators. II: Rings, Disks and Rods of Arbitrary Profile," J. Sound Vibration **6**, 351–364 (1967).
[13] C. Kusakabe and M. Konno, "Piezoelectric Mechanical Filter for Low Frequencies," J. Inst. Elect. Comm. Japan **51-A**, 40–41 (1968).

Appendix A

$$\mathbf{H}=\int_0^1 (\mathbf{X}''\mathbf{X}''^T)dy=\mathbf{U}\bar{\mathbf{H}}\mathbf{U}, \tag{A1}$$

where

$$\bar{\mathbf{H}}=\begin{bmatrix} 12 & 6 & -12 & 6 \\ 6 & 4 & -6 & 2 \\ -12 & -6 & 12 & -6 \\ 6 & 2 & -6 & 4 \end{bmatrix} \tag{A2}$$

and

$$\mathbf{J}=\int_0^1 (\mathbf{X}\mathbf{X}^T)dy=\mathbf{U}\bar{\mathbf{J}}\mathbf{U}, \tag{A3}$$

where

$$\bar{\mathbf{J}}=\frac{1}{420}\begin{bmatrix} 156 & 22 & 54 & -13 \\ 22 & 4 & 13 & -3 \\ 54 & 13 & 156 & -22 \\ -13 & -3 & -22 & 4 \end{bmatrix} \tag{A4}$$

and

$$\mathbf{U}=\begin{bmatrix} 1 & 0 & 0 & 0 \\ 0 & r_{Li} & 0 & 0 \\ 0 & 0 & 1 & 0 \\ 0 & 0 & 0 & r_{Li} \end{bmatrix}, \tag{A5}$$

and

$$\mathbf{D}=\mathbf{E}^T\mathbf{E}, \tag{A6}$$

where

$$\mathbf{E}=[0,\ -r_{Li},\ 0,\ r_{Li}], \tag{A7}$$

$$\mathbf{U}_c=\mathbf{U}\,|_{r_{Li}=r_{Loj}}, \tag{A8}$$

$$\mathbf{K}=\int_0^1 (\mathbf{X}_\theta'\mathbf{X}_\theta'^T)dy=\begin{bmatrix} 1 & -1 \\ -1 & 1 \end{bmatrix}, \tag{A9}$$

and

$$\mathbf{M}=\int_0^1 (\mathbf{X}_\theta\mathbf{X}_\theta^T)dy=\frac{1}{6}\begin{bmatrix} 2 & 1 \\ 1 & 2 \end{bmatrix}. \tag{A10}$$